

See discussions, stats, and author profiles for this publication at: <https://www.researchgate.net/publication/231662696>

# Liquid Structure of Acetonitrile–Water Mixtures by X-ray Diffraction and Infrared Spectroscopy

ARTICLE in THE JOURNAL OF PHYSICAL CHEMISTRY B · OCTOBER 1998

Impact Factor: 3.3 · DOI: 10.1021/jp9824297

CITATIONS

173

READS

178

4 AUTHORS, INCLUDING:



Toshiyuki Takamuku

Saga University

84 PUBLICATIONS 1,922 CITATIONS

SEE PROFILE



Masaaki Tabata

Saga University

123 PUBLICATIONS 1,831 CITATIONS

SEE PROFILE



Jun Nishimoto

Hiroshima Prefectural University

32 PUBLICATIONS 520 CITATIONS

SEE PROFILE

# Liquid Structure of Acetonitrile–Water Mixtures by X-ray Diffraction and Infrared Spectroscopy

Toshiyuki Takamuku, Masaaki Tabata,\* Atsushi Yamaguchi, and Jun Nishimoto

Department of Chemistry, Faculty of Science and Engineering, Saga University,  
Honjo-machi, Saga 840-8502, Japan

Midori Kumamoto

Department of Food and Nutrition, Faculty of Home Science, Nishikyushu University,  
Kanzaki-machi, Saga 842-8585, Japan

Hisanobu Wakita and Toshio Yamaguchi

Department of Chemistry, Faculty of Science, Fukuoka University, Nanakuma,  
Jonan-ku, Fukuoka 814-0180, Japan

Received: June 1, 1998; In Final Form: August 13, 1998

The structure of acetonitrile–water mixtures has been investigated by X-ray diffraction with an imaging plate detector and IR spectroscopy over a wide range of acetonitrile mole fractions ( $0.0 \leq X_{AN} \leq 1.0$ ). Reichardt  $E_T^N$  and Sone-Fukuda  $D_{II,I}$  values were also measured for the mixtures. It has been found from the X-ray data that in pure acetonitrile an acetonitrile molecule interacts with two nearest neighbors by antiparallel dipole–dipole interaction together with a small shift of the two molecular centers and that two acetonitrile molecules in the second-neighbor shell interact with a central molecule through parallel dipole–dipole interaction. Thus, acetonitrile molecules are alternately aligned to form a zigzag cluster. On addition of water into pure acetonitrile, water molecules interact with acetonitrile molecules through a dipole–dipole interaction in an antiparallel orientation. The IR spectra of O–D and C≡N stretching vibrations, observed for mixtures of acetonitrile AN and water containing 20% D<sub>2</sub>O, suggested that hydrogen bonds are also formed between acetonitrile and water molecules in the mixtures at  $X_{AN} \leq 0.8$ . The average numbers of the first- and second-neighbor acetonitrile molecules gradually increase with increasing water content with an almost constant first-neighbor distance and slightly decreased second-neighbor ones. Thus, acetonitrile molecules are assembled to form three-dimensionally expanded clusters; the acetonitrile clusters are surrounded by water molecules through both hydrogen bonding and dipole–dipole interaction. The X-ray radial distribution functions and IR spectra suggest that the hydrogen bond network of water is enhanced in the mixtures at  $X_{AN} < 0.6$ . The concentration dependence of  $E_T^N$  and  $D_{II,I}$  values determined reflects well the above-mentioned behavior of water molecules in the mixtures. These findings suggest that both water and acetonitrile clusters coexist in the mixtures in the range of  $0.2 \leq X_{AN} < 0.6$ , i.e., “microheterogeneity” occurs in the acetonitrile–water mixtures.

## Introduction

Acetonitrile (AN)–water (H<sub>2</sub>O) mixtures at various mole fractions are widely used in many fields such as liquid chromatography, solvent extraction, organic synthesis, and electrochemistry. For example, the acetonitrile–water mixture can extract highly charged ion pair complexes that cannot be extracted into conventional organic solvents such as chloroform.<sup>1</sup> Acetonitrile has unique characteristics, e.g., high dielectric constant (35.95) and solubilization of many inorganic and organic materials.<sup>2</sup> In addition, acetonitrile is one of aprotic solvents which are miscible in water at any ratio similar to dimethyl sulfoxide and acetone. Furthermore, acetonitrile molecules do not strongly interact with themselves, while water molecules form a hydrogen bond network. Previous X-ray

diffraction studies<sup>3–6</sup> on pure acetonitrile pointed out that acetonitrile molecules are weakly associated through dipole–dipole interaction.

Much attention has been paid to the physicochemical properties of acetonitrile–water mixtures. Several studies have been conducted on the thermodynamic, spectroscopic, transport, and electrochemical properties of acetonitrile–water mixtures. The viscosity of the acetonitrile–water mixture at an ambient temperature<sup>7</sup> shows a maximum at an acetonitrile mole fraction of  $X_{AN} = 0.1$ . A phase separation of the acetonitrile–water mixture<sup>8</sup> occurs at 272 K at  $X_{AN} = 0.38$ . Moreover, the self-diffusion coefficients of water and acetonitrile molecules<sup>9,10</sup> are equal at  $X_{AN} = 0.75$ . Excess Gibbs free energies of mixing<sup>11,12</sup> and enthalpies of mixing<sup>13</sup> were also measured, and their anomalies discussed frequently. Ben-Naim<sup>14</sup> and Marcus<sup>15</sup> suggested homo- and heteromolecular interactions in various mixtures of water and organic solvents from the values of

\* Corresponding author. Phone: +81-952-28-8560. Fax: +81-952-28-8548. E-mail: tabatam@cc.saga-u.ac.jp.

Kirkwood–Buff integrals. Molecular dynamics simulation<sup>16</sup> and dynamic properties<sup>17</sup> have suggested the structure of microheterogeneity that contains clusters of one type of molecules, either CH<sub>3</sub>CN or H<sub>2</sub>O when an acetonitrile content is sufficiently high. This term, “microheterogeneity,” describes the situation in which molecules of each of the components are preferentially surrounded by molecules of the same kind. On the basis of measurements of Kamlet and Taft’s parameters (KT’s  $\pi^*$ ;  $\alpha$ ;  $\beta$ ) and theoretical calculations, Marcus and Migron<sup>18</sup> concluded that microheterogeneity sets in at  $X_{\text{AN}} \geq 0.33$  and the acetonitrile molecule is solvated by water at low mole fractions of acetonitrile.

Recently IR spectroscopic studies on acetonitrile–water mixtures were carried out by Jamroz et al.<sup>19</sup> and Bertie and Lan.<sup>20</sup> Jamroz et al.<sup>19</sup> measured the C≡N stretching band of CD<sub>3</sub>CN–H<sub>2</sub>O mixtures and the O–D stretching band of diluted HOD in CH<sub>3</sub>CN–H<sub>2</sub>O with ca. 8% HDO. They concluded that molecular arrangement in the mixture is remarkably nonrandom by strong preferential solvation. Bertie and Lan<sup>20</sup> determined the concentrations of both hydrogen-bonded and free water and acetonitrile species from integrated intensities as areas under the O–H and C≡N bands. They suggested the existence of microheterogeneity at compositions near  $X_{\text{AN}} = 0.3$ – $0.5$  and of 58% of hydrogen-bonded water at  $X_{\text{AN}} = 0.2$ . Kasende and Zeegers-Huyskens<sup>21</sup> estimated the formation constant of acetonitrile–water adduct (1:1) in CCl<sub>4</sub> by the IR spectroscopic method. Wakisaka et al.<sup>22,23</sup> confirmed the formation of clusters in acetonitrile–water mixtures by mass spectrometry and suggested the formation of acetonitrile-hydrate clusters, H<sup>+</sup>(CH<sub>3</sub>CN)(H<sub>2</sub>O)<sub>16–26</sub>, H<sup>+</sup>(CH<sub>3</sub>CN)<sub>2</sub>(H<sub>2</sub>O)<sub>14–16</sub>, and H<sup>+</sup>(CH<sub>3</sub>CN)<sub>3</sub>(H<sub>2</sub>O)<sub>12–22</sub>.

As described above, a change in liquid structure with the mole fraction of acetonitrile has been discussed frequently on the basis of indirect structural information such as thermodynamic parameters and viscosity. However, few reports have clarified the microheterogeneity and anomalies of various physicochemical properties of the acetonitrile–water mixture at a molecular level by means of neutron and X-ray diffraction. In the present study X-ray diffraction measurements were performed on acetonitrile–water mixtures over the wide range of acetonitrile mole fraction ( $0.0 \leq X_{\text{AN}} \leq 1.0$ ) to obtain direct structural information on cluster formation in the mixtures. The nature of molecular association also was investigated by IR spectroscopic measurements of the O–D and C≡N stretching bands of HDO and CH<sub>3</sub>CN, respectively, in the mixtures of CH<sub>3</sub>CN and H<sub>2</sub>O containing 20% D<sub>2</sub>O. In addition, the  $E_{\text{T}}^{\text{N}}$  and  $D_{\text{II,1}}$  values<sup>24,25</sup> were measured by UV spectrophotometry to estimate electron donicity and acceptability of constituent solvent molecules in the mixtures. Finally, we propose structure models of clusters formed in the mixtures at various mole fractions of acetonitrile and discuss a possible origin of anomalous behaviors in physicochemical properties from the direct structural evidence obtained. This is the first report directly clarifying the microstructure of acetonitrile–water mixtures at the atomic level over the wide range of the acetonitrile mole fraction.

## Experimental Section

**Reagents.** Acetonitrile (Wako Pure Chemicals, Extra grade) was dried with thermally activated 4-Å molecular sieves and then distilled under a nitrogen atmosphere. Acetonitrile–water mixtures were prepared by weighing the acetonitrile and distilled water to desired mole fractions of acetonitrile. The densities of the solutions were measured at 25 °C with a densimeter (ANTON Paar K.G. DMA 35).

**X-ray Diffraction Measurements.** All X-ray diffraction measurements for pure acetonitrile and water and their mixtures at  $X_{\text{AN}} = 0.1, 0.2, 0.25, 0.38, 0.4, 0.6, 0.75$ , and  $0.8$  were made at room temperature (25 °C) on a rapid X-ray diffractometer combined with an imaging plate (IP) detector (MAC Science Co., Ltd. DIP301). Details of the diffractometer and its performance have been described previously.<sup>26,27</sup> X-rays were generated at a rotary Mo anode operated at 50 kV and 200 mA, and then monochromatized by a graphite crystal to obtain Mo  $K\alpha$  radiation ( $\lambda = 0.7107$  Å). A sample solution was sealed in a glass capillary with a 1-mm inner diameter and measured in transmission geometry. The observed range of the scattering angle ( $2\theta$ ) was  $0.2^\circ$  to  $109^\circ$ , corresponding to the scattering vector ( $s = 4\pi\lambda^{-1}\sin\theta$ ) of  $0.03$  to  $14.4$  Å<sup>−1</sup>. An exposure time for X-rays was 3 h per sample solution.

Two-dimensional data,  $I_{\text{obsd}}(x, y)$ , on IP were integrated into one-dimensional data,  $I_{\text{obsd}}(\theta)$ , by a method reported previously.<sup>26,27</sup> The observed intensities were corrected for background,<sup>27</sup> absorption in a sample and cell,<sup>27</sup> and polarization<sup>28</sup> and then normalized to absolute units in a usual manner.<sup>29–31</sup> The structure function,  $i(s)$ , is given by

$$i(s) = KI_{\text{obsd}}(s) - \sum x_j f_j^2(s) \quad (1)$$

where  $K$  represents a normalization factor of the observed intensities,  $I_{\text{obsd}}(s)$ , to absolute units,  $x_j$  is the number of atom  $j$  in a stoichiometric volume,  $V$ , containing one N atom for acetonitrile and acetonitrile–water mixtures and one O atom for water, and  $f_j(s)$  is the atomic scattering factor of atom  $j$  corrected for the anomalous dispersion. The scattering factors for neutral atoms were taken from the International Tables for X-ray Crystallography.<sup>32</sup> The  $i(s)$  values weighed by  $s$  are Fourier transformed into the radial distribution function,  $D(r)$ , as

$$D(r) = 4\pi r^2 \rho_0 + \frac{2r}{\pi} \int_0^{s_{\text{max}}} si(s) M(s) \sin(rs) ds \quad (2)$$

Here,  $\rho_0 (= [\sum x_j f_j(0)]^2/V)$  stands for the average scattering density of a sample solution and  $s_{\text{max}}$  is a maximum  $s$  value attained in the measurements ( $s_{\text{max}} = 14.4$  Å<sup>−1</sup>). The modification function,  $M(s)$ , has a form

$$M(s) = [\sum x_j f_j^2(0)/\sum x_j f_j^2(s)] \exp(-ks^2) \quad (3)$$

with a damping factor,  $k$ , being chosen as  $0.01$  Å<sup>2</sup> in the present case.<sup>33</sup> A comparison between the experimental structure function and theoretical one based on a model was made by a least-squares refinement procedure of minimizing an error square sum.

$$U = \sum_{s_{\text{min}}}^{s_{\text{max}}} s^2 \{i_{\text{obsd}}(s) - i_{\text{calcd}}(s)\}^2 \quad (4)$$

The theoretical intensity,  $i_{\text{calcd}}(s)$ , was calculated by

$$i_{\text{calcd}}(s) = \sum_i \sum_j x_i n_{ij} f_i(s) f_j(s) \frac{\sin(r_{ij}s)}{r_{ij}s} \exp(-b_{ij}s^2) - \sum_i \sum_j x_i x_j f_i(s) f_j(s) \frac{4\pi R_j^3 \sin(R_j s) - R_j s \cos(R_j s)}{V (R_j s)^3} \times \exp(-B_j s^2) \quad (5)$$

The first term of the right-hand side of eq 5 is related to the short-range interactions characterized by the interatomic distance  $r_{ij}$ , the temperature factor  $b_{ij}$ , and the number of interactions  $n_{ij}$  for atom pair  $i-j$ . The second term arises from the interaction between a spherical hole and the continuum electron distribution beyond the hole.  $R_j$  is the radius of the spherical hole around atom  $j$ , and  $B_j$  is the softness parameter for emergence of the continuum electron distribution.

All X-ray diffraction data were analyzed by the programs KURVLR<sup>28</sup> and NIPLSQ.<sup>34</sup>

**IR Measurements.** Acetonitrile–water mixtures used for IR measurements were prepared by mixing CH<sub>3</sub>CN with H<sub>2</sub>O containing 20% D<sub>2</sub>O. The sample solution was kept in a cell with CaF<sub>2</sub> windows separated with a Teflon spacer. The O–D and C≡N stretching bands for HDO and CH<sub>3</sub>CN in the mixtures at various mole fractions of acetonitrile were measured at room temperature (25 °C) from 2000 to 3000 cm<sup>-1</sup> on an Fourier transform IR spectrophotometer (Perkin-Elmer SPECTRUM 2000).

**Measurements of  $E_T^N$  and  $D_{II}$  Values.** The values of parameters  $E_T^N$  and  $D_{II}$  were determined for acetonitrile–water mixtures at various mole fractions of acetonitrile by the literature methods described by Reichardt<sup>24</sup> and Sone and Fukuda,<sup>25</sup> respectively. Indicators used were 2,6-diphenyl-4-(2,4,6-triphenylpyridinio)phenoxide (DTP) in the former case and bis-(2,4-pentanediolato)oxovanadium(IV) (VO(acac)<sub>2</sub>) in the latter. UV visible absorption spectra of the sample solutions were measured at room temperature on a UV visible spectrophotometer (JASCO V-550). First, an  $E_T(30)_S$  value for each sample was determined from a relation  $E_T(30)_S/\text{kJ mol}^{-1} = 1.196 \times 10^5/\lambda$ , where  $\lambda$  denotes the wavelength of absorption maximum observed for the sample solutions. Then, the normalized  $E_T^N$  value was calculated by a relation  $E_T^N = (E_T(30)_S - E_T(30)_{\text{TMS}})/(E_T(30)_W - E_T(30)_{\text{TMS}})$ , where  $E_T(30)_W$  and  $E_T(30)_{\text{TMS}}$  denote the values for water (264 kJ mol<sup>-1</sup>) and tetramethylsilane (128 kJ mol<sup>-1</sup>), respectively.<sup>24</sup> The  $D_{II}$  value was obtained from the relation  $D_{II}/\text{kJ mol}^{-1} = 1.196 \times 10^5/(\lambda_{II} - \lambda_I)$ , where  $\lambda_I$  and  $\lambda_{II}$  denote the wavelengths of the absorption maxima.

## Results and Discussion

**X-ray Diffraction.** The  $s$ -weighted structure functions obtained for pure acetonitrile and water and acetonitrile–water mixtures at various mole fractions of acetonitrile are shown in Figure 1. The corresponding radial distribution functions (RDFs) in the form of  $D(r) - 4\pi r^2 \rho_0$  are shown in Figure 2.

**Structure of Pure Acetonitrile.** The predominant peaks are observed around 1.2, 2.6, and 3–5 Å in the RDF for pure acetonitrile ( $X_{\text{AN}} = 1.0$ ). The first two peaks are mainly assigned to intramolecular C<sub>1</sub>–N and C<sub>1</sub>–C<sub>2</sub> interactions and nonbonding C<sub>2</sub>...N interaction within an acetonitrile molecule (see Figure 3 for symbols C<sub>1</sub>, C<sub>2</sub>, and N). The third broad peak at 3–5 Å corresponds to the interactions between nearest neighbor acetonitrile molecules.

As for the intermolecular structure, Kratochwill et al.<sup>3</sup> considered all possible interactions among eight acetonitrile molecules within an assumed orthorhombic unit cell and proposed a model that all molecules are arranged so that the dipoles of acetonitrile molecules are directed in either parallel or antiparallel directions. Bertagnoli and co-workers<sup>4,5</sup> concluded from a combined neutron and X-ray diffraction experiment of liquid acetonitrile that the dipole–dipole and quadrupole–quadrupole interactions are essential at short intermolecular distances and that the antiparallel orientation of the dipoles is preferred between the first neighbors. Radnai et al.<sup>6</sup> also

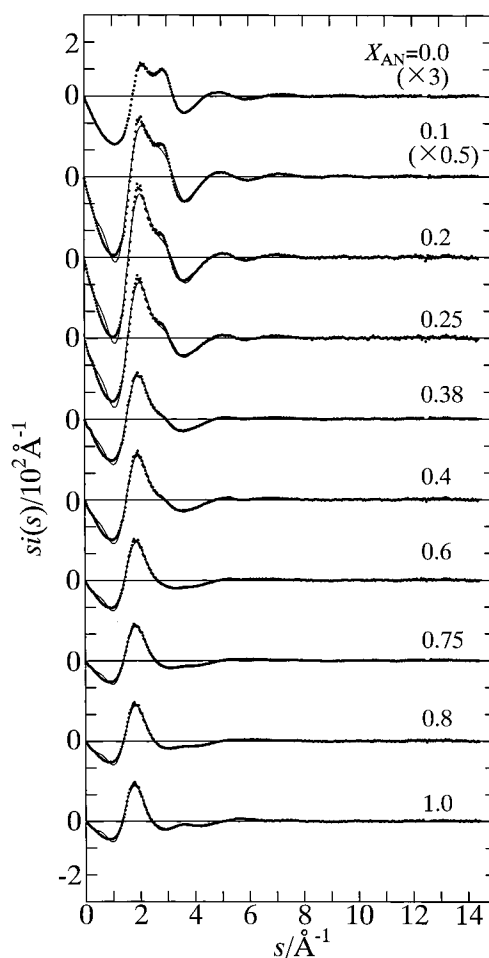


**Figure 1.** Structure functions  $i(s)$  multiplied by  $s$  for pure acetonitrile and water and the acetonitrile–water mixtures at the various acetonitrile mole fractions,  $X_{\text{AN}}$ . The dotted and solid lines are experimental and calculated ones, respectively.

proposed that two acetonitrile neighbors be arranged in an antiparallel direction around a central molecule from an X-ray diffraction measurement of liquid acetonitrile. They estimated the distance between the molecular centers as  $l = 3.30$  Å. They assumed that acetonitrile molecules beyond the two nearest neighbors are randomly distributed.

In the present analysis, it has been found that the broad peak at 3–5 Å in the RDF was explained well only when both antiparallel and parallel dipole–dipole orientations are assumed for the first-neighbor and the second-neighbor molecules, respectively, as proposed by Kratochwill et al.<sup>3</sup> It has also been found that the dipole centers of the first-neighbor molecules are shifted by 1.47 Å from a central molecule. A small broad peak observed at distances  $r \geq 6.5$  Å suggested no significant long-range structure due to the dipole–dipole interaction in pure acetonitrile. Thus, the 6.5-Å peak was not analyzed in the present analysis; instead, an even electron distribution was assumed for the long-range interaction beyond 6 Å.

To perform a quantitative analysis the least-squares fitting procedure was applied to the structure function over the  $s$ -range from 0.1 to 14.4 Å<sup>-1</sup>. The intramolecular structure parameters for an acetonitrile molecule previously determined from the X-ray diffraction experiment by Radnai et al.<sup>6</sup> were used in the subsequent analysis. The optimized values of structure parameters are summarized in Table 1. Figure 3 shows the most likely structure for pure acetonitrile proposed from the present X-ray diffraction data. As shown in a side view of Figure 3,



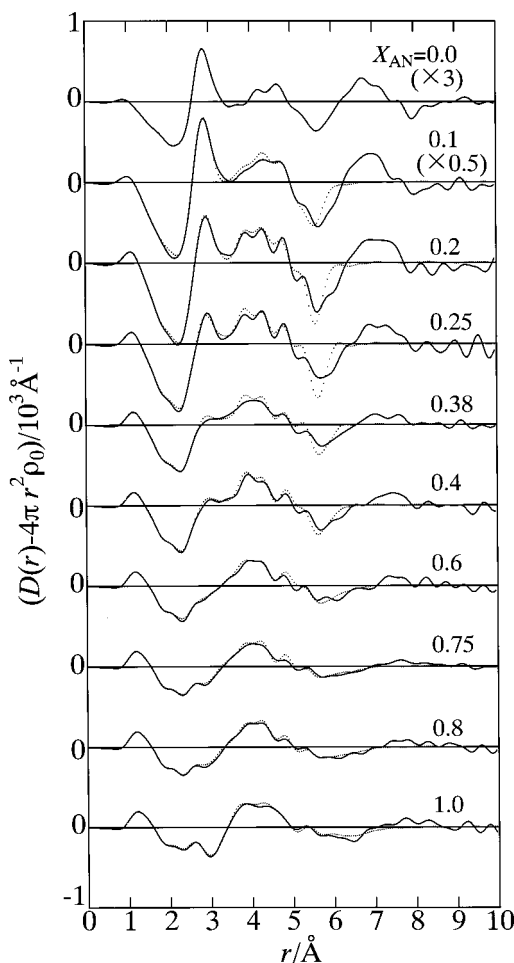


**Figure 2.** Radial distribution functions in the form of  $D(r) - 4\pi r^2 \rho_0$  for pure acetonitrile and water and the acetonitrile–water mixtures at various acetonitrile mole fractions,  $X_{AN}$ . The solid and dotted lines are experimental and calculated ones, respectively.

acetonitrile molecules are alternately aligned to form a zigzag cluster. The distances between the first-neighbor molecules is 3.45 Å ( $C_1 \cdots N'$  and  $N \cdots C_1'$ ), and the dipole centers are shifted by 1.47 Å for the  $C_1$ – $C_2$  bond length. The number of the first-neighbor acetonitrile molecules is 2.0 (1). The distance and number of the second-neighbor molecules in parallel are 4.10 (3) Å and 2.0 (1), respectively. It is likely that such arrangements are repeated to form a zigzag cluster consisting of 4–6 acetonitrile molecules. As seen in Figures 1 and 2, the theoretical  $si(s)$  and RDF calculated with the optimized values in Table 1 reproduced well the experimental values except for the long-range part at  $s < 1.5 \text{ Å}^{-1}$  and  $r \geq 6 \text{ Å}$ , respectively, not taken into account in the present analysis.

**Structure of Acetonitrile–Water Mixtures.** As seen in Figure 2, the RDFs at  $X_{AN} = 0.6, 0.75$ , and  $0.8$  do not drastically change by addition of water to pure acetonitrile, except that a hollow around 3.0 Å in the RDF at  $X_{AN} = 1.0$  gradually disappears with decreasing acetonitrile concentration. To better clarify the change of RDFs, the differential radial distribution functions (DRDFs) were calculated by subtracting the RDF of pure acetonitrile ( $X_{AN} = 1.0$ ) from those of the mixtures at  $0.8 \geq X_{AN} \geq 0.1$  (Figure 4). As seen in Figure 4, a peak around 3.0 Å can be observed in the DRDF at  $X_{AN} = 0.8$ , together with a tail at a longer distance. When the water content increases this peak increases and shifts toward the peak of the  $O \cdots H-O$  hydrogen bond (2.85 Å) at  $X_{AN} = 0.0$ . Consequently, the peak at 3.0 Å and its tail probably arise from the interactions between

acetonitrile and water molecules due to antiparallel dipole–dipole interaction on the basis of their large dipole moments and van der Waals radii. From a consideration that an oxygen atom of a water molecule is placed by 3.00 Å ( $C_1 \cdots O$ ) above the  $C_1$  atom of an acetonitrile molecule, the  $C_2 \cdots O$  and  $N \cdots O$  distances are estimated to be 3.34 and 3.21 Å, respectively. This model well explains the interactions around 3.0–3.4 Å in the RDFs of the mixtures at  $X_{AN} = 0.6, 0.75$ , and  $0.8$ .

Further addition of water to the mixtures brings a new peak at 2.85 Å in the RDFs at  $X_{AN} \leq 0.4$  (Figure 2). The new peak arises mainly from formation of hydrogen bonds among water molecules in the mixtures. Many authors have suggested  $N \cdots H-O$  hydrogen bonds between acetonitrile and water molecules,<sup>19,20</sup> and we also confirmed the hydrogen bonds from IR measurements as described in the next section. However, the RDFs could not give strong evidence for formation of such a hydrogen bond because  $N \cdots H-O$  bonds are not distinguishable from  $O \cdots H-O$  hydrogen bonds between water molecules owing to the similar X-ray scattering power of N and O atoms and comparable bond lengths. Hence, the following hydrogen bond model was adopted in the present analysis. The model is characterized by linear  $CN \cdots HO$  hydrogen bonds with  $N \cdots O$ ,  $C_1 \cdots O$ , and  $C_2 \cdots O$  distances of 2.80, 3.95, and 5.42 Å and temperature factors of 0.01, 0.02, and 0.02 Å<sup>2</sup>, respectively. According to the IR spectroscopic study by Bertie and Lan,<sup>20</sup> the concentration ratios of hydrogen-bonded acetonitrile molecules to total acetonitrile molecules were estimated to be 0.80, 0.58, 0.54, 0.47, 0.45, 0.31, 0.22, and 0.18 at  $X_{AN} = 0.1, 0.2, 0.25, 0.38, 0.4, 0.6, 0.75$ , and  $0.8$ , respectively. The differential RDFs were then obtained by subtracting the contribution of both intramolecular interactions and acetonitrile–water hydrogen bonds from the total RDF. A typical differential RDF obtained at  $X_{AN} = 0.4$  is given in Figure 5. As seen in Figure 5, most of the peaks in the  $r$  range of 2.8–5.5 Å still remain in the differential RDF, showing a small contribution of hydrogen bonds between acetonitrile and water molecules to the total RDF. In addition, the differential RDF shows that the acetonitrile–acetonitrile interaction observed for pure acetonitrile still remains in the mixture. The interactions around 3.0 Å are also observed in the differential RDF at  $X_{AN} = 0.4$ , suggesting again that acetonitrile molecules are hydrated by water molecules through the dipole–dipole interaction. These trends were also observed in all differential RDFs in the range of  $0.2 \leq X_{AN} \leq 0.8$ . However, as seen in Figure 2, the total RDF at  $X_{AN} = 0.1$  is comparable to that for pure water except a small broad peak at 3.9–4.0 Å. The interaction of acetonitrile and acetonitrile molecules contributes to the RDF to a small extent.

The peak at 2.85 Å in Figure 2 gradually grows with increasing water content. A new peak around 7 Å, due mainly to the third-neighbor  $O \cdots O$  interactions in hydrogen-bonded network, also increases with increasing water content at  $X_{AN} \leq 0.4$ . This result suggests that the water–water hydrogen-bonded network is enhanced in the acetonitrile–water mixtures in this  $X_{AN}$  range. In the total RDFs obtained at  $0.2 \leq X_{AN} \leq 0.4$ , three peaks at 3.9–4.0, 4.2–4.4, and 4.8 Å, predominantly arising from the second-neighbor acetonitrile–acetonitrile interactions such as  $C_1 \cdots C_1'$ ,  $C_1 \cdots C_2'$ , and  $N \cdots C_2'$ , were sharpened with increasing water content; this result suggests that the acetonitrile–acetonitrile interactions are also strengthened in the mixtures. On the contrary, these peaks disappear in the RDF at  $X_{AN} = 0.1$ , suggesting breaking of acetonitrile–acetonitrile clusters.

From the present finding that dipole–dipole interaction among acetonitrile molecules observed for pure acetonitrile

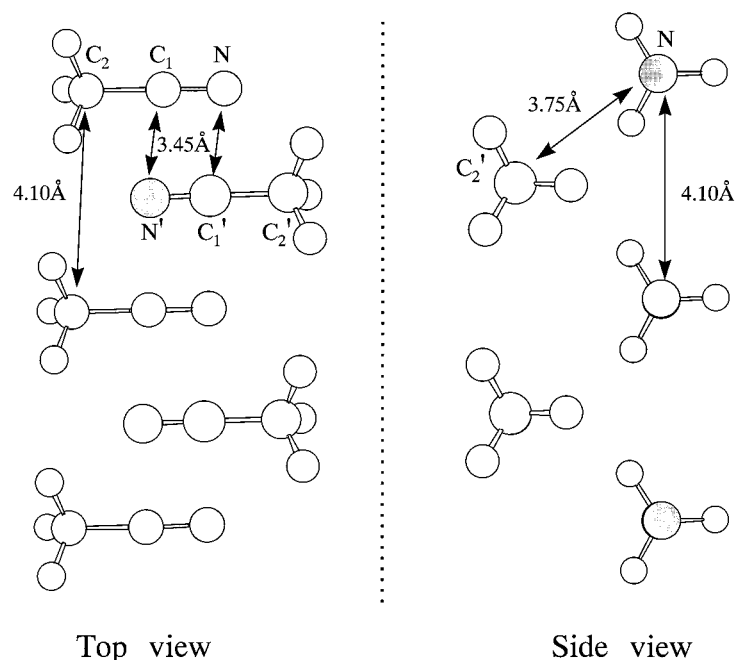


**Figure 3.** Proposed cluster structure of pure acetonitrile. A central acetonitrile molecule interacts with two nearest neighbors at 3.45 Å in antiparallel and 4.10 Å in parallel.

**TABLE 1: Important Parameter Values of the Interactions in Acetonitrile and Acetonitrile–Water Mixtures at Various Acetonitrile Mole Fractions Obtained from the Least-Squares Fits<sup>a</sup>**

		$X_{AN}$								
interaction	parameter	0.1	0.2	0.25	0.38	0.4	0.6	0.75	0.8	1.0
First Neighbor AN...AN										
$C_1 \cdots C_1'$	$r$	3.74 (2)	3.65 (3)	3.62 (3)	3.63 (1)	3.68 (2)	3.65 (2)	3.67 (1)	3.69 (2)	3.64 (2)
	$10^3b$	5	20	20	20	20	20	20	20	30
	$n$	4.4 (6)	3.9 (4)	3.8 (5)	3.4 (1)	3.3 (2)	2.0 (1)	2.1 (1)	2.1 (1)	2.0 (1)
$N \cdots C_1'$	$r$	3.50	3.50	3.50	3.50	3.50	3.50	3.50	3.50	3.45
	$10^3b$	5	15	15	15	15	20	20	20	30
	$n$	7.2	7.2	7.2	6.0	6.0	4.0	4.0	4.0	4.0
Second Neighbor AN...AN										
$N \cdots N'$	$r$	3.96	3.96	3.96	3.96	3.96	4.00	4.00	4.00	4.10
	$10^3b$	5	12	12	12	12	12	12	12	60
	$n$	3.6	3.6	3.6	3.0	3.0	2.0	2.0	2.0	2.0
$C_1 \cdots C_1'$	$r$	3.98 (3)	4.04 (3)	3.99 (3)	4.00 (1)	3.98 (2)	4.01 (2)	4.00 (1)	3.99 (2)	4.10 (3)
	$10^3b$	5	12	12	12	12	12	12	12	60
	$n$	4.0 (5)	3.2 (4)	3.9 (4)	3.2 (1)	3.3 (2)	2.2 (2)	2.0 (1)	2.0 (1)	2.0 (1)
AN...H <sub>2</sub> O Dipole–Dipole Interaction										
$C_1 \cdots O$	$r$	2.99 (2)	3.00 (2)	3.02 (2)	3.003 (7)	3.018 (9)	3.02 (1)	2.993 (6)	2.98 (1)	
	$10^3b$	20	20	20	20	20	20	20	20	
	$n$	2.1 (2)	2.0 (1)	2.0 (1)	1.50 (5)	1.65 (6)	0.98 (5)	0.97 (3)	0.96 (3)	
H <sub>2</sub> O...H <sub>2</sub> O Hydrogen Bond										
$O \cdots O$	$r$	2.842 (2)	2.849 (3)	2.847 (5)	2.852 (3)	2.855 (4)	2.859 (14)			
	$10^3b$	19	20	20	20	20	10			
	$n$	3.26 (4)	2.80 (4)	2.80 (4)	2.62 (4)	2.60 (6)	1.20 (8)			

<sup>a</sup> The interatomic distance  $r$ (Å), the temperature factor  $b$ (Å<sup>2</sup>), and the number of interactions  $n$  per acetonitrile molecule. The values in parentheses are estimated standard deviations of the last figure. The parameters without standard deviations were not allowed to vary in the calculations.

exists even in acetonitrile–water mixtures at  $0.2 \leq X_{AN} \leq 0.8$ , a model fitting on the RDFs for the mixtures was made in a trial-and-error manner by modifying the structure parameters for the zigzag cluster in pure acetonitrile and by including the parameters for acetonitrile–water interactions and water–water hydrogen bonds. Then, by using the structural models thus obtained, the least-squares fitting procedure was applied to the structure functions for the acetonitrile–water mixtures over the  $s$ -range of 0.1 to 14.4 Å<sup>−1</sup>; the optimized values are summarized in Table 1. The distances (3.45–3.50 Å) of the first-neighbor acetonitrile–acetonitrile interaction ( $C_1 \cdots N'$  or  $N \cdots C_1'$ ) do not significantly change between pure acetonitrile and mixtures,

whereas the number of the first-neighbor acetonitrile molecules gradually increases from 2.0 (1) at  $X_{AN} = 1.0$  to 3.9 (4) at  $X_{AN} = 0.2$  with increasing water content. On the other hand, the distance of the second-neighbor acetonitrile molecules was shortened slightly from 4.10 (3) Å for the pure acetonitrile to 3.98 (2) – 4.04 (3) Å for the acetonitrile–water mixtures. The number of the second-neighbor interaction increases from 2.0 (1) for pure acetonitrile to 2.0 (1) – 3.9 (4) for the mixtures. The distance of dipole–dipole interaction ( $C_1 \cdots O$ ) between acetonitrile and water molecules falls within a range of 2.98 (1) – 3.02 (2) Å in the range of  $0.2 \leq X_{AN} \leq 0.8$ . The number of the dipole–dipole interaction gradually increases from 0.96

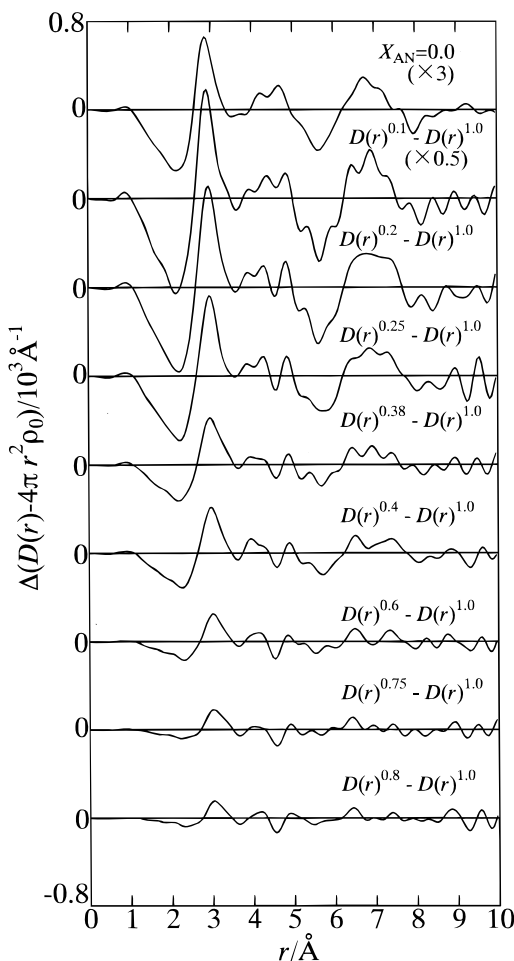


**Figure 4.** Differential radial distribution functions (DRDFs) obtained from the RDFs shown in Figure 2, together with the RDF for pure water (upper) for comparison.

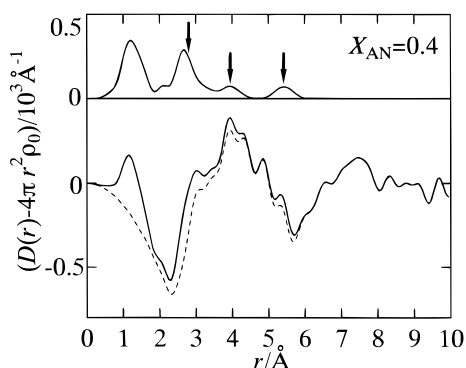


**Figure 5.** Radial distribution function originated from hydrogen bonding between acetonitrile and water molecules (upper) and the observed (solid line) and residual (dashed line) radial distribution functions at  $X_{AN} = 0.4$  (lower). The arrows correspond to the positions of  $N\cdots O$ ,  $C_1\cdots O$ , and  $C_2\cdots O$  interactions in acetonitrile–water hydrogen bond.

(3) at  $X_{AN} = 0.8$  to 2.0 (1) at  $X_{AN} = 0.2$  when the water content increases. Unfortunately, the structure parameters for the hydrogen bond between acetonitrile and water molecules could not be refined because of its small contribution to the RDFs. Thus, the structure parameters of the hydrogen bond were fixed in the model. On the other hand, the number of the first-neighbor water–water hydrogen bond gradually increases from 1.20 (8) at  $X_{AN} = 0.6$  to 2.80 (4) at  $X_{AN} = 0.2$  with increasing water content, but the formation of water–water hydrogen bond

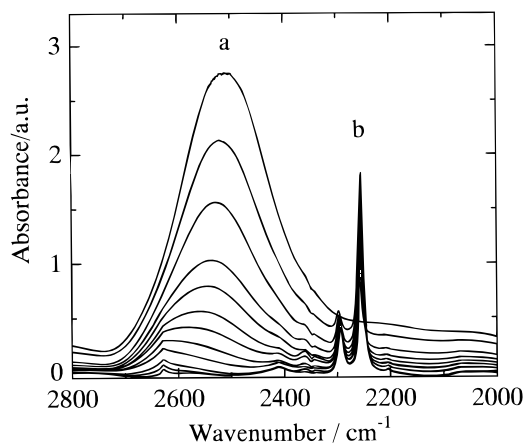


**Figure 6.** IR absorption spectra of (a) HDO and (b)  $CH_3CN$  in the mixtures of acetonitrile with water containing 20%  $D_2O$  at various mole fractions of acetonitrile:  $X_{AN} = 0.00, 0.09, 0.20, 0.30, 0.40, 0.50, 0.60, 0.70, 0.80, 0.95$ , and 1.00 from the top to the bottom of the IR absorption spectra.

was not observed for the mixtures at  $X_{AN} = 0.75$  and 0.8. The number of the first-neighbor water–water hydrogen bond, 3.26 (4), at  $X_{AN} = 0.1$  is comparable to that, 3.1, for bulk water.<sup>26</sup> Both theoretical  $si(s)$  and RDFs, calculated by use of the optimized values in Table 1, well reproduced the observed values as seen in Figures 1 and 2.

The X-ray diffraction measurements for the acetonitrile–water mixtures suggest that the zigzag clusters as shown in pure acetonitrile remain even in the mixtures at low water contents. In the mixtures water molecules interact with acetonitrile molecules on the surface of cluster through antiparallel dipole–dipole interaction. However, X-ray diffraction measurements could not clarify the formation of acetonitrile–water hydrogen bond. When water is added further to acetonitrile, acetonitrile molecules tend to gather to form three-dimensional clusters rather than to distribute randomly. Moreover, water molecules form hydrogen-bonded networks in the mixtures at  $X_{AN} \leq 0.4$ . Thus, both acetonitrile and water clusters coexist in the acetonitrile–water mixtures in the range of  $0.2 \leq X_{AN} < 0.6$ . However, the RDF at  $X_{AN} = 0.1$  indicates that acetonitrile clusters are disrupted in the mixture.

**IR Spectra.** Figure 6 shows IR spectra in the wavenumber range of 2000–2800  $cm^{-1}$  measured for pure acetonitrile and water and mixtures of acetonitrile with water containing 20%  $D_2O$  at various acetonitrile concentrations. Three bands appear in the spectra for the mixtures. The major band around 2500–2640  $cm^{-1}$  is attributed to the O–D stretching mode of HDO molecules. Two sharp bands arising from the vibration modes within acetonitrile molecule are observed at 2257 and 2295  $cm^{-1}$ . The large band at 2257  $cm^{-1}$  originates from the  $C\equiv N$  stretching mode ( $\nu_2$ ), and the other band around 2295  $cm^{-1}$  is a combination band of both  $CH_3$  bending ( $\nu_3$ ) and  $C-C$  stretching ( $\nu_4$ ) modes.<sup>19</sup> In the present study, the  $C\equiv N$  stretching mode was used as a probe of formation of hydrogen bond between acetonitrile and water molecules.

The wavenumbers for both O–D and  $C\equiv N$  stretching modes were plotted against the mole fraction of acetonitrile in Figure 7a,b, respectively. As seen in Figure 7a, the wavenumber of the O–D stretching mode gradually decreases with a decrease in  $X_{AN}$  or an increase in water content. This is because the O–D bonds of the water molecule will be weakened by formation of a water–water hydrogen bond in the mixtures. In particular, the wavenumber linearly decreases with decreasing mole fraction of acetonitrile from  $X_{AN} \approx 0.7$ –0.4, revealing

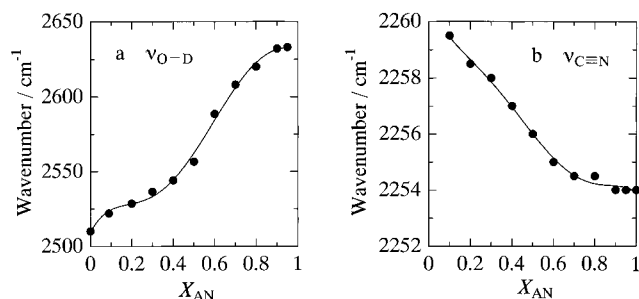


**Figure 7.** Wavenumbers for (a) O–D and (b) C≡N stretching bands vs the mole fraction of acetonitrile  $X_{AN}$ . The error is  $0.5\text{ cm}^{-1}$  in wavenumber.

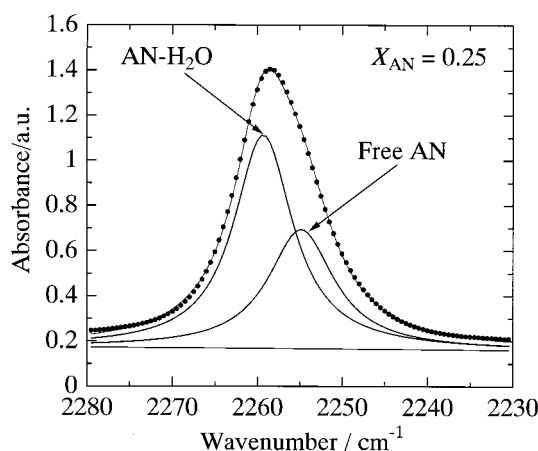


**Figure 8.** Deconvoluted C≡N stretching band of  $\text{CH}_3\text{CN}$  in the acetonitrile–water mixtures with two Lorentzians and a linear baseline at  $X_{AN} = 0.25$ : experimental (dots), each component band (solid line) for the interaction of hydrogen-bonded (AN– $\text{H}_2\text{O}$ ) and free acetonitrile molecules, and calculated sum of both components (solid line overlapped on dots).

that the water–water hydrogen bonds are enhanced in the mixtures at  $X_{AN} \leq \sim 0.7$ . The trend agrees with that from the present X-ray diffraction experiments.

The wavenumber of the C≡N stretching mode increases as the water content increases as seen in Figure 7b. Jamroz et al.<sup>19</sup> investigated  $\text{CD}_3\text{CN}$ – $\text{H}_2\text{O}$  mixtures by IR spectroscopy and showed that the  $\nu_2$  mode of C≡N stretching in the  $\text{CD}_3\text{CN}$ – $\text{H}_2\text{O}$  mixtures consists of two bands at 2263 and ca. 2267  $\text{cm}^{-1}$  assignable to free and hydrogen-bonded  $\text{CD}_3\text{CN}$  molecules, respectively. Furthermore, they indicated that the 2263  $\text{cm}^{-1}$  band from free  $\text{CD}_3\text{CN}$  molecules consists of three Lorentzians due to an overlap of hot band transitions. In the present study of  $\text{CH}_3\text{CN}$ , the C≡N stretching band at 2257  $\text{cm}^{-1}$  could be deconvoluted into two Lorentzians at 2254 and 2259  $\text{cm}^{-1}$  as shown in Figure 8. The former is assigned to free acetonitrile molecules because this band is observed for pure  $\text{CH}_3\text{CN}$ . The latter band at 2259  $\text{cm}^{-1}$  is observed only for the mixtures, and thus attributed to hydrogen-bonded acetonitrile molecules. When the water content was varied, the intensities of the two Lorentzians drastically changed, but their wavenumbers did not change significantly.

In Figure 9, the area normalized by the acetonitrile concentration for each component at 2254 and 2259  $\text{cm}^{-1}$  is plotted against the mole fraction of acetonitrile. The amount of free acetonitrile molecules is almost constant in the range of  $0.7 \leq X_{AN} \leq 1.0$  and gradually decreases with increasing water content at  $0.1 \leq X_{AN} < 0.7$ , whereas the extent of hydrogen-bonded acetonitrile molecules rapidly increases with decreasing  $X_{AN}$

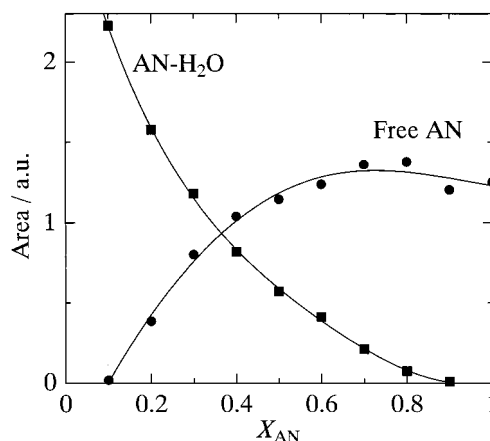


**Figure 9.** Concentration dependence of the areas normalized by acetonitrile concentration for the resolved IR component bands ascribed to hydrogen-bonded (AN– $\text{H}_2\text{O}$ ) and free acetonitrile.

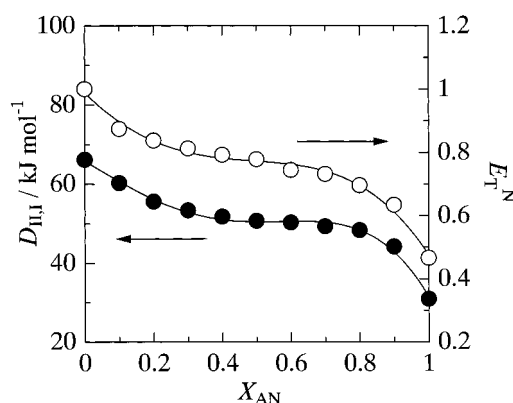


**Figure 10.** Values of  $E_T^N$  (opened circle) and  $D_{II,I}/\text{kJ mol}^{-1}$  (filled circle) values vs the mole fraction of acetonitrile  $X_{AN}$ .

from  $\sim 0.8$ . These trends are comparable with the IR spectroscopic study by Bertie and Lan.<sup>20</sup>

On the basis of the IR results together with those from X-ray diffraction, acetonitrile clusters are gradually surrounded by water molecules through both hydrogen bond and dipole–dipole interaction with increasing water content in the range of  $0.2 \leq X_{AN} < 0.8$ .

**$E_T^N$  and  $D_{II,I}$  Values.** The  $E_T^N$  and  $D_{II,I}$  values determined are depicted against the mole fraction of acetonitrile in Figure 10. The  $E_T^N$  value<sup>24</sup> is used as a probe of electron acceptability of a solvent molecule and has a linear correlation with the Gutmann–Mayer acceptor number.<sup>35</sup> On the other hand, the  $D_{II,I}$  value<sup>25</sup> reflects both electron donicity and acceptability of a solvent molecule because this parameter is related to solvation of both oxygen and vanadium atoms within  $\text{VO}(\text{acac})_2$  complex by acceptor and donor atoms of the solvent molecules, respectively. In the case of acetonitrile–water mixtures, both  $E_T^N$  and  $D_{II,I}$  values will predominantly reflect the acceptability of water molecule rather than that of acetonitrile since water has a larger acceptor number (54.8) than acetonitrile (19.3) with comparable donor numbers of water (18) and acetonitrile (14.1). Thus, water molecule can preferentially hydrate the probe atoms by its strong acceptor atom of proton.

When ideal mixing occurs in acetonitrile–water mixtures, both  $E_T^N$  and  $D_{II,I}$  values should change linearly with the mole fraction of acetonitrile. However, both values decrease similarly with increasing  $X_{AN}$ , accompanying with two inflection points at  $X_{AN} \approx 0.2$  and  $0.8$ . This tendency is very similar to a change in vapor pressures of acetonitrile–water mixtures;<sup>36</sup>



e.g., the vapor pressure of water is almost constant in a range of  $0.4 \leq X_{\text{AN}} < 0.7$ . The anomalies at  $X_{\text{AN}} \approx 0.2$  and  $0.8$  can be explained as follows. Addition of water into acetonitrile leads to a rapid increase of both  $E_{\text{T}}^{\text{N}}$  and  $D_{\text{II,I}}$  values in the range of  $0.8 < X_{\text{AN}} \leq 1.0$  because of preferential solvation of water molecule. With further increase in water content these values moderately increase in the range of  $0.2 \leq X_{\text{AN}} \leq 0.8$ . In this range water molecules interact with acetonitrile and water molecules by dipole–dipole interaction and hydrogen bonding; thus, concentration of water molecules that can interact with the probe atoms increases moderately. On further addition of water at  $X_{\text{AN}} \leq 0.2$ , the interaction between water and acetonitrile molecules decreases in the mixtures, leading to the rapid increase of both  $E_{\text{T}}^{\text{N}}$  and  $D_{\text{II,I}}$  values. At high water contents ( $X_{\text{AN}} < 0.2$ ), acetonitrile clusters are broken, and water clusters become predominant in the mixtures as discussed in the X-ray diffraction section.

Although both  $E_{\text{T}}^{\text{N}}$  and  $D_{\text{II,I}}$  parameters originally reflect the donor–acceptor properties for pure solvent, but not those for mixed solvents, the above changes in both values well support the results from X-ray diffraction and IR spectroscopy as described before. This is probably because the strong acceptability of water molecule mainly governs the donor–acceptor properties of the acetonitrile–water mixtures.

**Cluster Structures and Enthalpy of Mixing.** The RDF obtained for pure acetonitrile has revealed that four to six acetonitrile molecules form a cluster of zigzag structures through both antiparallel and parallel dipole–dipole interactions. On addition of water to acetonitrile, water molecules interact with the acetonitrile cluster through dipole–dipole interaction at  $X_{\text{AN}} \leq 0.8$ . The IR data on the  $\text{C}\equiv\text{N}$  stretching mode of an acetonitrile molecule have shown that hydrogen bonds between acetonitrile and water molecules form in the mixtures at  $X_{\text{AN}} \leq 0.8$  and that the amount of hydrogen-bonded acetonitrile molecules gradually increases in the mixture with increasing water content. However, it has been found from the X-ray diffraction data that the acetonitrile clusters remain over the range of  $0.2 \leq X_{\text{AN}} \leq 0.8$ . In particular, acetonitrile molecules are assembled to form three-dimensionally expanded clusters with decreasing  $X_{\text{AN}}$  to  $0.2$ . On the other hand, the RDFs have shown that water–water hydrogen-bonded network is gradually enhanced in the mixtures at  $X_{\text{AN}} \leq 0.4$ , but almost disappear at  $0.6 \leq X_{\text{AN}} \leq 0.8$ . At  $X_{\text{AN}} \geq 0.6$  the translational motion of the water molecule will increase to be comparable with that of acetonitrile molecule because of breaking hydrogen bonds among water molecules. Thus, the self-diffusion coefficients of water and acetonitrile<sup>9,10</sup> are equal at  $X_{\text{AN}} = 0.75$ . The IR spectroscopic data for the O–D stretching mode of HDO molecule in the mixtures have supported that water–water hydrogen bonds are evolved in the mixtures at  $X_{\text{AN}} < \sim 0.7$ . Therefore, it is concluded from combined X-ray and IR data that each of the component molecules tends to associate with the same molecular species rather than with unlike molecule and that both clusters of water and acetonitrile coexist, that is, “microheterogeneity” occurs in the mixtures in the range of  $0.2 \leq X_{\text{AN}} < 0.6$ . The dipole–dipole interaction and hydrogen bonding between acetonitrile and water molecules probably serve to form an interface between both clusters in the mixtures. An actual phase separation to two liquid phases occurs for an acetonitrile–water mixture at  $X_{\text{AN}} = 0.38$  when interfacial water molecules are embedded into the enhanced hydrogen-bonded network at an undercooled temperature (272 K).<sup>8</sup> On the contrary, in the mixtures at  $X_{\text{AN}} < 0.2$  the acetonitrile clusters are disrupted, and the hydrophobic hydration will be strengthened around acetonitrile molecules. Hence, the viscosity of

acetonitrile–water mixture<sup>7</sup> shows a maximum at  $X_{\text{AN}} = 0.1$ . The mole fraction dependence of the  $E_{\text{T}}^{\text{N}}$  and  $D_{\text{II,I}}$  values determined for the mixtures well reflects such a behavior of water molecules in the whole range of acetonitrile concentration.

Many authors have discussed anomalies in physicochemical properties of acetonitrile–water mixtures from various macroscopic information. However, the present direct structural evidence for cluster formation can more clearly explain the change in the enthalpy of mixing with the mole fraction of acetonitrile at room temperature. The enthalpies of mixing<sup>13</sup> are largely positive over most of concentration range, accompanied by a maximum ( $\Delta H^{\text{E}} \approx 1.1 \text{ kJ mol}^{-1}$ ) at  $X_{\text{AN}} \sim 0.6$ . The large positive values are mainly attributed to the breaking of hydrogen bonds among water molecules, although the dipole–dipole interaction among acetonitrile molecules contributes slightly to the change in the enthalpy value. In the range of  $\sim 0.6 \leq X_{\text{AN}} < 1.0$ , water molecules will interact with acetonitrile molecules mainly on the surface of acetonitrile clusters and do not form hydrogen bonds among themselves; thus, the enthalpy value gradually increases with increasing water content. At  $X_{\text{AN}} < 0.6$ , on the contrary, enthalpy arising from formation of hydrogen bonds among water molecules is generated in the mixtures; hence, the enthalpy value gradually decreases with increasing water content. Although the acetonitrile clusters are disrupted in the mixtures at  $X_{\text{AN}} < 0.2$ , the water–water hydrogen-bonded network is enhanced enough to cancel out a loss of enthalpy for break-down of the acetonitrile cluster. The cluster models proposed here reasonably explain the mole fraction dependence of the enthalpy of mixing with the unique maximum at  $X_{\text{AN}} \sim 0.6$ .

## Conclusions

The present study suggests how an aprotic molecule dissolves in water. In the case of acetonitrile–water mixtures, the dipole–dipole interaction between water and acetonitrile molecules plays an important role in mixing of acetonitrile in water at any ratio. In acetonitrile–water mixtures both acetonitrile and water clusters coexist; thus, microheterogeneity occurs in the mixtures. If acetonitrile molecules are replaced with water molecules into the hydrogen bond network of water, the microheterogeneity does not occur, and the enthalpies of mixing could not be positive. In fact, the enthalpies of mixing for methanol–water mixtures at room temperature are negative over the whole range of alcohol concentration. The microheterogeneity is a key to a homogeneous solvent extraction and liquid chromatography, in which a solute is in equilibrium between acetonitrile and water clusters.

**Acknowledgment.** The present work was supported in part by a Grant-in-Aid for Encouragement of Young Scientists (No. 09740444) (T.T.), a Grant-in-Aid B (No. 08454238) (M.T.), and a Grant-in-Aid B (No. 09440207) (T.Y.) from the Ministry of Education, Science, Sports and Culture, Japan.

## References and Notes

- (1) Tabata, M.; Kumamoto, M.; Nishimoto, J. *Anal. Chem.* **1996**, *68*, 758.
- (2) Riddick, J. A.; Bungh, W. B.; Sakano, T. K. *Organic Solvents*, 4th ed.; John Wiley & Sons: New York, 1986.
- (3) Kratochwill, A.; Weidner, J. U.; Zimmermann, H. *Ber. Bunsen-Ges. Phys. Chem.* **1973**, *77*, 408.
- (4) Bertagnolli, H.; Zeidler, M. D. *Mol. Phys.* **1978**, *35*, 177.
- (5) Steinhauser, O.; Bertagnolli, H. *Chem. Phys. Lett.* **1981**, *78*, 555.
- (6) Radnai, T.; Itoh, S.; Ohtaki, H. *Bull. Chem. Soc. Jpn.* **1988**, *61*, 3845.
- (7) Moreau, C.; Douhéret, G. *Thermochim. Acta* **1975**, *13*, 385.

- (8) Schneider, G. Z. *Physik. Chem. N. F.* **1964**, 41, 327.  
(9) Easteal, A. J. *Austr. J. Chem.* **1980**, 33, 1667.  
(10) Hawlicka, E. Z. *Naturforsch.* **1988**, 43a, 769.  
(11) Villamanan, M. A.; Van Ness, H. C. *J. Chem. Eng. Data* **1985**, 30, 445.  
(12) French, H. T. *J. Chem. Thermodyn.* **1987**, 19, 1155.  
(13) Stokes, R. H. *J. Chem. Thermodyn.* **1987**, 19, 977.  
(14) Ben-Naim, A. *Pure Appl. Chem.* **1990**, 62, 25.  
(15) Marcus Y. *J. Chem. Soc., Faraday Trans.* **1990**, 86, 2215.  
(16) Kovacs, H.; Laaksonen, A. *J. Am. Chem. Soc.* **1991**, 113, 5596.  
(17) Goldammer, E.; Hertz, H. G. *J. Phys. Chem.* **1970**, 74, 3734.  
(18) Marcus, Y.; Migron, Y. *J. Phys. Chem.* **1991**, 95, 400.  
(19) Jamroz, D.; Stangret, J.; Lingdren, J. *J. Am. Chem. Soc.* **1993**, 115, 6165.  
(20) Bertie, J. E.; Lan, Z. *J. Phys. Chem. B* **1997**, 101, 4111.  
(21) Kasende, O.; Zeegers-Huyskens, T. *Spectrosc. Lett.* **1980**, 13, 493.  
(22) Wakisaka, A.; Shimizu, Y.; Nishi, N.; Tokumaru, K.; Sakuragi, H. *J. Chem. Soc., Faraday Trans.* **1992**, 88, 1129.  
(23) Wakisaka, A.; Takahashi, S.; Nishi, N. *J. Chem. Soc., Faraday Trans.* **1995**, 91, 4063.  
(24) Reichardt, C. *Solvents and Solvent Effects in Organic Chemistry*; Verlag Chemie: Weinheim, 1988.  
(25) Sone, K.; Fukuda, Y. *Inorganic Thermochemistry*; Springer: New York, 1987.  
(26) Yamanaka, K.; Yamaguchi, T.; Wakita, H. *J. Chem. Phys.* **1994**, 101, 9830.  
(27) Ihara, M.; Yamaguchi, T.; Wakita, H.; Matsumoto, T. *Adv. X-Ray Anal. Jpn.* **1994**, 25, 49.  
(28) Johanson, G.; Sandström, M. *Chem. Scr.* **1973**, 4, 195.  
(29) Furukawa, K. *Rep. Prog. Phys.* **1962**, 25, 395.  
(30) Krogh-Moe, J. *Acta Crystallogr.* **1956**, 2, 951.  
(31) Norman, N. *Acta Crystallogr.* **1957**, 10, 370.  
(32) International Tables for X-ray Crystallography, Vol. 4; Kynoch Press: Birmingham, 1974.  
(33) Takamuku, T.; Yamaguchi, T.; Wakita, H. *J. Phys. Chem.* **1991**, 95, 10098.  
(34) Yamaguchi, T. Doctoral Thesis, Tokyo Institute of Technology, 1978.  
(35) Gutmann, V. *The Donor-Acceptor Approach to Molecular Interactions*; Plenum Press: New York, 1978.  
(36) de Landsberg, V. *Bull. Soc. Chim. Belg.* **1940**, 49, 59.